Influence of MWCNT morphology on dispersion and thermal properties of polyethylene nanocomposites

Influence of MWCNT morphology on dispersion and thermal properties of polyethylene nanocomposites.

Silvia Barus[1], Pierangiola Bracco[1], Simone Musso[2], Angelica Chiodoni[3], Alberto Tagliaferro[4], Marco Zanetti[1*]

[1]*IFM Chemistry Department and Nanostructured Interface and Surface (NIS) Centre of Excellence, Università degli Studi di Torino, via Pietro Giuria 7, 10125 Torino, Italy*

[2]*Department of Physics, Politecnico di Torino, Corso Duca degli Abruzzi 24, 10129 Torino Italy*

[3]*Department of Materials and Microsystems Laboratory, Politecnico di Torino, Corso Duca degli Abruzzi 24, 10129 Torino Italy*

[4]*Department of Material Science and Chemical Engineering, Politecnico di Torino, Corso Duca degli Abruzzi 24, 10129 Torino Italy*

* Corresponding author:
Tel.: +39-011-670-7554; fax: +39-011-670-7855.
E-mail address: marco.zanetti@unito.it (M. Zanetti).

Abstract

In this study a series of melt mixed multi-walled carbon nanotube (MWCNTs)/Polyethylene (PE) composites with different kind and several concentrations of carbon nanotubes (CNTs) were investigated. The morphology and degree of dispersion of the fillers in the polymer matrix at different length scales was investigated using scanning electron microscopy (SEM) and transmission electron microscopy (TEM). Both individual and agglomerations of MWCNTs were evident but a good dispersion was observed for some of them. TGA measurements were performed on nanocomposites in order to understand if CNTs affect the stabilisation mechanism during thermal and oxidative degradation. The analysis demonstrate that MWCNT presence slightly delays thermal volatilisation (15–20°C) without modification of thermal degradation mechanism. Whereas thermal oxidative degradation in air is delayed up to about 100°C dependently from MWCNT concentration, in the range used here (0.1–2.0 wt.%), and degree of dispersion . The stabilisation is due to the formation of a thin protective layer of entangled MWCNTs kept together by carbon char generated on the surface of the nanocomposites as shown by SEM images taken on degradation residues.

Keywords: polyethylene (PE), multiwalls carbon nanotubes (MWCNT), thermal degradation, thermoxidation, dispersion.

1 INTRODUCTION

Carbon nanotubes (CNTs) are graphitic sheets rolled into seamless tubes (i.e., arrangements of carbon hexagons into tube-like fullerenes) having a diameter ranging from about a nanometer to tens of nanometers with lengths up to centimetres. Both theoretical and experimental studies have shown CNTs to have extremely high tensile moduli (>1 TPa for single walled carbon nanotubes, SWCNTs) and tensile strengths of the order of 500 GPa [1,2]. Carbon nanotubes are thermally stable up to over 2400°C in vacuum, have a thermal conductivity along their principal axes about double than that of diamond and electric-current-carrying capacity up to 1000 times higher than copper wire. Due to their extraordinary mechanical, electrical and optical properties together with their low density(1.3-2.4 g/cm^3), CNTs have attracted great attention in recent years in the field of composites materials. As the structure and properties of the CNTs have been understood, there is a pressing need to transfer their outstanding properties from nano to micro/macro-scales. One essential step towards this goal is their processing, which often involves dispersing them in a polymeric matrix to form complex materials such as polymer-CNTs nanocomposites. These composites represent the first realized major commercial application of CNTs [3]. Researchers have used many different techniques to attempt an efficient dispersion of nanotubes in polymer matrices, including functionalization of nanotubes surface [4-9], use of polymers to coat the nanotubes surface [10], in situ polymerization [11,12], ultrasonic dispersion in solution [13,14], melt processing [15-20], use of surfactants [9,21], electrospinning [22]. Irrespective of the method of preparation there are three fundamental and critical issues associated with transferring the unique properties of carbon nanotubes to a polymer matrix. Firstly, the nanotubes must be uniformly distributed and well dispersed throughout the polymer matrix, secondly, there must be enhanced interfacial interaction between the polymer and the nanotubes and, finally, some types of CNTs, such as single walled and/or defect free ones, have high cost. The last problem is essential from the application point of view. Thus, it is important not only to obtain a final product exhibiting good performances but also to use small amount of low-cost CNTs. Incorporation of CNTs into polymers dramatically enhances the mechanical properties of the material [23,24] and it also imparts attractive properties such as conductivity, electromagnetic interference shielding and sensing capability to the otherwise inert polymer matrix [3,25]. The outstanding improvement of physical properties with carbon nanotubes is in part attributed to their extremely high aspect ratio (length to outer diameter ratio) of up to 1000. An improvement in flammability properties of polymers has been obtained with nanoscale additives and these filled systems provide an alternative to conventional flame retardants. At present, the most common approach is the use of layered silicates

having large aspect ratios; the flame retardant (FR) effectiveness of clay/polymer nanocomposites with various resins has been demonstrated [26-31]. The FR effectiveness in polymethylmethacrylate of nanoscale silica particles (average diameter of 12 nm) has also been demonstrated [32]. Carbon nanotubes provide another candidate as an FR additive because of their highly elongated shape; as a matter of fact CNTs were already used to reduce flammability properties of several polymer materials, showing a general reduction of combustion rate [33,34]. There is another practical advantage for dispersing carbon nanotubes in PE compared with dispersing clay or silica into polyolefins. Since clay and silica are hydrophilic, they often require (i) an organic treatment on their surfaces and/or (ii) a compatibilizing polymer modifier, e. g. PE grafted with MA [35]. On the other hand, carbon nanotubes are organophilic and can be dispersed directly into the polymer without a previous treatment.

In this study, we have examined the effect that the CNTs dispersion has on thermal properties and on the morphology of PE-based nanocomposites. Multiwall carbon nanotubes (MWCNTs) are used due to their cost advantage over single wall carbon nanotubes. We report the preparation of different composites, changing type of CNTs (from very perfect to defective ones), using melt blending technique, in order to evaluate how they can influence the material behaviour.

2 EXPERIMENTAL SECTION

2.1 Materials

Not stabilized low density polyethylene, PE, Riblene® FM-50 (density of 0,933 g/cm^3, method ASTM D 1505, melting point of 118°C and melt flow index 3.5 g/10 min, method ASTM D 1238 at 190°C/2,16 Kg) produced and kindly provided in grains form by Polimeri Europa, was used as matrix for this work. Three different MWCNTs samples have been used as filler. Their salient characteristics are reported in the table 1. Henceforth, the Nano Carbon MWCNT will be designated as αCNTs; the Nano Amor ones as βCNTs and the Carbon Group ones like γCNTs.

2.2 Composites preparation

Composites of PE filled with different amount (from 0.1% to 2 wt%) of CNTs were prepared by melt compounding at 160°C using a Brabender internal mixer AEV330. The manufacturing temperature was kept at 160°C and the screw speed amounted to 50 rpm for 10 min. All samples were then compression moulded at 180±5°C, under a pressure of 100 bars for 5 min to obtain 50x50x10 mm plates. Samples of pristine PE were moulded in the same conditions to be used as references. For the convenience of this discussion, the different samples are denoted by these

abbreviations: for example, PE nanocomposites filled with αCNTs at 0.1wt% is named PEαCNT0.1.

2.3 Sample characterization

The morphology of different types of CNTs was studied recording images on a JEOL 3010-UHR TEM, operating at an accelerating voltage of 300 kV. Samples were placed onto carbon-coated copper grids. The distribution of MWCNTs inside the composites was studied recording images on chemically etched cryo-fractured samples with a Zeiss Supra 40 field emission scanning electron microscope (FESEM) after a chrome plating carried out by a Baltec SCD 050, working in argon atmosphere in vacuum with a 60 mA current for 60 sec, to obtain a gilt deposition of about 20-30 nm of Cr. The chemical etching was performed in a strong oxidant mixture of H_2SO_4, H_3PO_4, $KMnO_4$. Samples were kept in the mixture at room temperature, for 2 hours in order to remove the amorphous fracture line and make visible the microcrystalline structure of the material [38].

Thermal degradation was measured on approx. 10 mg sample in a TGA Q500 balance, TA Inc., with alumina pan in a 100 cm^3/min nitrogen flow and with a 10°C/min heating ramp from room temperature up to 800°C. Thermo-oxidation was determined in the same way in a 100 cm^3/min air flow and with a 10°C/min heating ramp from room temperature up to 800°C.

Melt Flow Index, MFI, which is the output rate (flow) in grams that occurs in 10 minutes through a standard die when a fixed pressure is applied to the melt via a piston and a load of total mass of 2.16 kg at a temperature of 190°C (ASTM D-1238), was measured with a Extrusion Plastometer (ATS FAAR) on composite grains.

3 Result and Discussion

3.1 Aspect ratio and morphology of the MWCNT in PE

In fig. 1 are shown TEM and FESEM of the several types of nanotubes used in this work. In FESEM images, it is possible to distinguish the different morphologies and the level of aggregation of CNTs. αCNTs are completely disaggregated and it is possible to distinguish individual CNTs; βCNTs show an intermediate aggregation while γ are aggregated in mat formed by bundles (visible in the image). TEM images are useful to determine the degree of crystallinity: γ tubes show a bamboo structure, with open tips and presence of catalyst while αCNTs have parallel straight walls and closed tips; β ones have intermediate characteristics.

For the evaluation of the CNTs distribution within the polymer matrix, FESEM analysis has been used. Samples have been cryo-fractured and, subsequently, the fracture surface has been treated with a chemical etching in order to show up the lamellar crystalline microstructure. As we can see

in figure 2, the treatment is able to remove fracture line and roughness. In fig.2B is visible the PE typical microstructure. There are present spherulites which are aggregates with radial symmetry of crystalline lamellae.

As the various CNTs have different pristine morphology and characteristic dimension, we expected that the distribution and dispersion inside polymer matrix will be different. Experimental data validate our hypothesis as shown in figure 3. The white dots are CNTs aggregates (the smaller dots) or agglomerates (the bigger ones) while the filaments are isolated MWCNTs. Microscopic examination across the length scales would confirm that the perfect αCNTs (first column) are well distributed and dispersed in the PE matrix as isolated tubes and they don't aggregate even at high wt% of loading. The spherulitic microstructure is kept up to 0.1 wt% CNTs load. Some of the CNTs align in the flow direction, therefore, given sufficient wetting of the CNTs walls with the PE chains, the orientation of the CNTs may play a role in mechanical reinforcement. This is in contrast to polymer/CNT composites that are prepared by solution mixing, where the CNTs tend to be randomly oriented. The exhibited variation in the length of CNTs suggests that either (i) breakage of the nanotubes occurred during shear mixing or cryo-fracture, or (ii) the CNTs are extended below the surface. In the case of βCNTs (second column) we notice a good dispersion of tubes but some little aggregates are visible, starting from 0.5 wt% CNTs load. Notwithstanding the presence of aggregated tubes, most of them are isolated. As for αCNTs, the spherulic structure is maintained till 0.1 wt% CNTs load.

In the third column, the morphology of γCNTs loaded samples is completely different compared with the previous two: γCNTs are almost totally present in agglomerates, even at the lowest concentration. This is probably due to the fact that pristine CNTs were aggregated in mats and before being mixed with polymer were only smashed manually in a mortar. The larger agglomerates visible in the images are probably part of the original mat. Spherulites are visible at all loading till 1 wt% CNTs load. At higher loading, they disappear, indicating an effect of nanotube in the crystallization behaviour.

3.2 Thermal stability

Normalized weight loss curves measured in nitrogen atmosphere by TGA for the αCNT nanocomposite samples is plotted in figure 4. These results show that PE degrades with a large single peak starting around 400°C and that it is completely volatilized at 500°C. This large peak corresponds to the thermal degradation of PE initiated primarily by thermal scissions of C-C chain bonds, with a consequently formation of radical species, that decrease their molecular weight with depropagation and inter and intra-transfer reactions. The results for PE_αCNT samples also show

broad single peaks, but the temperatures at the peak sample weight loss rates are about 10-20°C higher than that of pure PE. For the range investigated in this study, the amount of CNT within PE does not significantly affect the thermal stability of this nanocomposite system in nitrogen. An increase in the temperature at the peak sample mass loss rate is also reported for the PP/PP-g-MA/clay system compared with PP/PP-g-MA [39]. This previous investigation indicated an increase of 17°C with 10 wt.% of clay in PP/ PP-g-MA. This effect was attributed to a barrier labyrinth effect of the clay platelets so that the diffusion of degradation products from the bulk of the polymer to the gas phase is slowed down. The temperature increase observed in the present study could arise from a similar barrier effect due to the hindered transport of degradation products caused by the numerous carbon tubes present in the sample.

Thermal degradation of the same samples in air is significantly different from that in nitrogen. The thermal stability of PE in air is prominently reduced by oxidative dehydrogenation accompanied by the formation of peroxy radicals that can decompose easily generating oxidized species. In fig. 5 a broad mass loss rate peak is observed for PE around 350°C. The thermal stability of the PE/ALPHA MWCNT nanocomposites appears to be higher than that of PE, indeed weight loss starts at higher temperatures. The stabilization becomes significant with already a percentage of filler of 0.5 wt%, where the mass loss starts around 350°C with an advantage in stability of about 50°C compared to PE alone. The TGA curves show a progressive stabilization to thermo-oxidation as CNT concentration increases insomuch as for the sample containing 2wt% the advantage is of about 100°C. As a matter of fact if we consider for example the weight % of different samples at the same temperature (430°C in our case) we can notice that for the polymer we have 12% of residue while for a 0.5wt% of CNT it is 52% and for the 2wt% sample is 81%, with only the 20% of the material volatilized. As regarding the nanocomposites containing the other types of CNT (curves not reported here), there is a concentration dependence on their stabilization for samples βCNT filled and no stability effect for the γCNT ones. The stabilization phenomena could be explained by the presence of CNT which can act, when present in suitable quantity, as physical protection.

Considering samples containing an equal wt% of CNT, the stability is promoted when filler has a good distribution in polymer matrix and improves when the dispersion get better, as in the case of α and β nanocomposites (figure 6). When CNT are present in bundles, as for γ nanocomposites, where a lot of them were trapped into aggregates, the movement of tubes is hindered and a protective layer can not be formed. If we consider the same samples, but in nitrogen atmosphere (figure 7), we can notice that filled samples show a little stabilization as compared to pure polymer and they all show the same behaviour in term of stabilization.

The burning process of a polymeric material typically begins with heating to a temperature at which thermal degradation initiates. The boiling temperatures of most of the thermal degradation products of polymers are much lower than the thermal degradation temperatures of thermoplastics, and the degradation products are then superheated and nucleated to form bubbles [40]. The bubbles burst at the heated surface evolving their contents into the gas phase as fuel vapor. One flame retardant approach is to suppress the bubbling rate, so as to reduce the supply rate of fuel by forming a protective and heat shielding char layer. A similar approach, that of forming a solid jammed network structure consisting of carbon nanotubes with tangled polymer chains has been demonstrated; this inhibits the otherwise vigorous bubbling process seen in the course of thermal degradation during combustion [41]. This previous study showed a close relationship between viscoelastic characteristics and the flammability properties of thermoplastic based polymer nanocomposites. In separate work, it has also been reported that the flammability of polymer–clay nanocomposites is reduced with an increase in melt viscosity and the formation of network [42,43].

In our study, the accumulation of CNT shaped into a network structure is observed as shown in figure 8. These images were obtained on cryo-fractured samples after a heating treatment in air with a ramp of 10°C/min up to 380°C. In the image with lower magnification we can see a progressive increase of CNT concentration going from the inner to the outer of material. On the image at higher magnification, we can notice a thick layer of entangled CNT stacked together by some carbonaceous material produced during polymer degradation. The formation of this tangled network (see figure on the right) tends to increase the mechanical integrity of the protective layer which could act also as a thermal insulator. Therefore the shielding effect derives from an ablative behaviour of the material: CNT migrate from the bulk of molten polymer to the surface, accumulating to form a shield, hindering the transport of degradation products from the bulk to the gas phase, thus stabilizing the material.

A qualitative measure of the viscosity of our nanocomposites was determined by MFI. The results are reported in fig. 9. In the graph we can notice that the melt flow decreases as the wt% of filler increases showing a change in the rheological properties of the materials. The decreasing of MFI entails that the viscosity of the systems increases with addition of the carbon nanotubes, indicating a transition from a liquid-like to a solid-like behavior due to the formation of a nanotube network which impedes the motion of polymer chains [44]. It is known from the literature that interconnected structures of anisometric fillers result in an apparent yield stress which is visible in dynamic measurements by a plateau of G′ or G″ versus frequency at low frequencies [45]. This effect is more pronounced in G′ than in G″. As the nanotube content increases in this composite system, nanotube–nanotube interactions begin to dominate, eventually lead to percolation and the

formation of an interconnected structure of nanotubes. Starting at about 2 wt% nanotubes, G′ seems to reach such a plateau at low frequencies. Therefore, an interconnected structure is assumed to form. Adding nanotubes, generally, causes a large energetic barrier for segmental motions of polymer chains in the confined space and thus increasing of the flow activation energy. In addition, Gu et al. [46] reported that strong interactions between polymer matrix and fillers may also cause greater activation energies of flow. The αCNT influence more this property because are the filler with the higher aspect ratio and are the more dispersed ones so their alignment in the flow is not easy.

In oxidant atmosphere, notice the greater stability reached, beyond the physical barrier behaviour, typical of other common nanocomposites (i.e. systems filled with layered silicates or silica nanoparticles) is possible that CNT act in other ways. According to previous data [47], a CNT may contain localised states, due to lattice defects, that can be considered as acceptor-like. The presence of acceptor-like electronic properties in CNT is mainly responsible for radical termination during polymer degradation, so CNT can actually act also as radical scavenger during the degradation in air where radical species are formed [48]. This phenomenon is visible in TGA curves, especially for samples filled with 2 wt% of CNT, at low temperature in the first phases of weight loss, where the curves have a "step trend" (see figure 5), typical of polymer containing antioxidants. Antioxidants species in polymer trap radicals, slowing down the subsequent formation of oxidized species. In our hypothesis the CNT could interfere with the formation of oxidized species just after the insertion of oxygen onto polymer chain (at about 200°C).

4 Conclusion

A melt processing method has been used to prepare polyethylene/MWCNTs nanocomposites. The CNTs were dispersed into the matrix by only the shearing action of a couple of screw without the use of compatibilizers. FESEM analyses have demonstrated that different types of CNTs were distributed in polymer matrix with different degrees of dispersion. As a consequence, the thermal properties of the composite were significantly affected by the dispersion efficiency. In fact, while samples with good distribution (obtained with both α and βCNTs) showed a better stabilization in air, as proven by TGA analyses, on the contrary, samples with a poor dispersion, containing γCNTs, don't show a stabilization effect to thermo-oxidation. The stabilization phenomenon is attributed to well dispersed CNTs into the polymer matrix. The nanotubes either form a physical shield on the surface of material, acting as an oxygen screening or decrease the formation rate of oxidized species.

In this work, good results in term of thermo-stability have been obtained even using βCNTs. These tubes are less purified and more defective than αCNTs but their dispersion and the resulting nanocomposite properties are comparable with the ones of samples containing the defect free CNTs. In conclusion, we also demonstrated that for potential application points of view, it is possible to consider the use of intermediate quality MWCNTs that require a cheaper production process.

Acknowledgment

Authors wish to thank Prof. Luigi Costa, University of Torino for helpful discussions and Dr.Luca Bertinetti, NIS Centre of Excellence for TEM measures.

References

1. Thostenson ET, Ren Z, Chou TW. Compos. Sci. Technol. 2001;61:1899-1912.
2. Lourie O, Cox DM, Wagner HD. Phys. Rev. Lett. 1998;81:1638-1641.
3. Baughman RH, Zakhidov AA, de Heer WA. Science 2002; 297:787-792.
4. Chen J, Hamon MA, Hu H, Chen Y, Rao AM, Eklund PC, Haddon RC. Science 1998; 282:95-98.
5. Mitchell CA, Bahr JL, Arepalli S, Tour JM, Krishnamoorti R. Macromolecules 2002; 35:8825-8830.
6. Bubert H, Haiber S, Brandl W, Marginean G, Heintze M, Bruser V. Diam. Relat. Mater. 2003; 12:811-815.
7. Eitan A, Jiang K, Dukes D, Andrews R, Schadler LS. Chem. Mater. 2003; 15:3198-3201.
8. Jang J, Bae J, Yoon SH. J. Mater. Chem. 2003; 13:676-681.
9. Shaffer MSP, Fan X, Windle AH. Carbon 1998; 36:1603-1612.
10. Star A, Stoddart JF, Steuerman D, Diehl M, Boukai A, Wong EW, Yang X, Chung SW, Choi H, Heath JR. Angew. Chem. Int. Ed. 2001; 40:1721-1725.
11. Jia Z, Wang Z, Xu C, Liang ., We B, Wu D, Zhu S. Mater. Sci. Eng. A 1999; 271:395-400.
12. Deng J, Ding X, Zhang W, Peng Y, Wang J, Long X, Li P, Chan ASC. Eur. Polym. J. 2002; 38:2497-2501.
13. Safadi B, Andrews R, Grulke EA. J. Appl. Polym. Sci. 2002; 84:2660-2669.
14. Qian D, Dickey EC, Andrews R, Rantell T, Appl. Phys. Lett. 2000; 76:2868-2870.
15. Jin Z, Pramoda KP, Xu G, Goh SH. Chem. Phys. Lett. 2001; 337:43-47.
16. Bhattacharyya AR, Sreekumar TV, Liu T, Kumar S, Ericson LM, Hauge RH, Smalley RE. Polymer 2003; 44:2373-2377.
17. Gorga RE, Cohen RE. J. Polym. Sci. Part. B: Polym. Phys. 2004; 42:2690-2702.
18. Potschke P, Bhattacharyya AR, Janke A. Eur. Polym. J. 2004; 40:137-148.
19. Siochi EJ, Working DC, Park C, Lillehei PT, Rouse JH,. Topping CC, Bhattacharyya AR, Kumar S, Composites B 2004; 35:439-446.
20. Tang WZ, Santare MH, Advani SG. Carbon 2003; 41:2779-2785.
21. Gong X, Liu J, Baskaran S, Voise RD, Young JS. Chem. Mater. 2000; 12:1049-1052.
22. Dror Y, Salalha W, Khalfin RL, Cohen Y, Yarin AL, Zussman E. Langmuir 2003; 19:7012-7026.
23. Tjong SC. Material Science and Engineering 2006; 53:73-197
24. Geng H, Rosen R, Zheng B, Shimoda H, Fleming L, Liu J, Zhou O. Adv. Mater. 2002; 14:1387-1390.
25. Sandler J, Shaffer MSP, Prasse T, Bauhofer W, Schulte K, Windle AH. Polymer 1999; 40:5967-5971.
26. Giannelis E. Adv. Mater. 1996; 8:29-35.
27. Gilman JW, Kashiwagi T, Lichtenhan JD.Proceedings 42th International SAMPE Symposium 1997; 1079-1089.
28. Gilman JW. Appl. Clay Sci. 1999; 15:31-49.
29. Zhu J, Morgan AB, Lamelas J, Wilkie CA. Chem. Mater. 2001; 13:3774-3780.
30. Zanetti M, Camino G, Mulhaupt R. Polym. Degrad. Stabil. 2001; 74:413-417.
31 Gilman JW, Jackson CL, Morgan AB, Harris R, Manias E, Giannelis EP, Wuthernow M, Hilton D, Phillips SH. Chem. Mater. 2000; 12:1866-73.
32. Kashiwagi T, Morgan AB, Antonoucci JM, VanLandingham MR, Harris RH, Awad WH, Shields JR. Journal of Applied Polymer Science 2003; 89:2072-2078.
33. Kashiwagi T, Grulke E, Hilding J, Harris R., Awad W, Douglas J. Macromol. Rapid Commun. 2002; 23:761-765.
34. Biercuk MJ, Llaguno MC, Radosavljevic M, Hyun JK, Johnson AT. Appl. Phys. Lett. 2002; 80:2767-2770.

35. Zanetti M, Bracco P, Costa L. Polymer Degradation and Stability 2004; 85: 657-665.
36. Kim YA, Hayashi T, Endo M, Kaburagi Y, Tsukada T, Shan J, Osato K, Tsuruoka S. Carbon 2005; 43:2243-2250.
37. Musso S, Fachini G, Tagliaferro A. Diamond & Related Materials 2005; 14:784-789.
38. Olley RH, Bassett DC. Polymer 1982; 23-28.
39. Zanetti M, Camino G, Reichert P, Muhaupt R. Macromol. Rapid. Commun. 2001; 22:176-180.
40. Kashiwagi T. Proc. Combust. Inst. 1994; 28:1423-1437.
41. Kashiwagi T, Du F, Douglas JF, Winey KI, Harris RH, Shields JR. Nat. Mater. 2005;4:928-933.
42. Bartholmai M, Schartel B. Polym. Adv. Technol. 2004;15:355-364.
43. Ma H, Tong L, Xu Z, Fang Z. Polym. Degrad. Stab. 2007;92:720-726.
44. Aalaie JL, Rahmatpour A, Maghami S. Journal of Macromolecular Science, Part B: Physics 2007; 46:877-889.
45. Utracki LA. Polymer Composites 1986; 7:274-282.
46. Gu SY, Ren J, Wang QF. J. Appl. Poly. Sci. 2004; 91:2427-2434.
47. Hsu WK, Chu SY, Munoz-Picone E, Boldu JL, Firth S, Franchi P, Roberts BP, Schilder A, Terrones H, Grobert N, Zhu YQ, Terrones M, McHenry ME, Kroto HW, Walton DRM. Chem. Phys. Lett. 2000; 323:572-579.
48. Watt PCP, Fearon PK, Hsu WK, Billingham NC, Kroto HW, Walton DRM. J. Mater. Chem. 2003; 13:491-495.

Captions

Table 1 Main characteristics of MWCNTs used in this work.

Figure 1 FESEM and TEM images of different types of CNTs.

Figure 2 FESEM images: fracture surface of PE before (A) and after (B) chemical etching.

Figure 3 FESEM images of etched cryo-fractured PE nanocomposites surfaces. Morphologies obtained with different weight percentages of CNTs.

Figure 4 TGA curves of PE nanocomposites filled with αCNTs in nitrogen atmosphere.

Figure 5 TGA curves of PE nanocomposites filled with αCNTs in air atmosphere.

Figure 6 TGA curves : comparison between the effect of different kind of CNTs (filled at 1 wt%) on the stabilization of material in air.

Figure 7 TGA curves : comparison between the effect of different kind of CNTs (filled at 1 wt%) on the stabilization of material in in nitrogen.

Figure 8 SEM image of nanocomposite samples heated at 380°C: lateral view (on the left) and top view (on the right).

Figure 9 MFI of different nanocomposites in function of wt% of filler.

	supplied by	nature	synthesis	characteristic dimension	Aspect*	purity	wt% catalyst **
α	Nano Carbon Technologies Co., Ltd., Akishima-Shi, Tokyo, Japan	commercial	floating reactant CCVD [36]	Diameter: 20-70 nm Length: dozen micron	very straight shape, little defective, facetted tips	> 98% (thermal annealing)	2
β	NanoAmor Inc., Houston, TX, USA	commercial	CCVD	Diameter: 50-80 nm Length: micron	intermediate defective	> 95%	4
γ	Carbon Group, Politecnico di Torino, Torino, Italy	experimental	CCVD [37]	Diameter: 40-80 nm Length: millimetres	mat shape, very defective, open tips	70-90%	6

Table 1

*determined by FESEM and TEM observation

**determined by TGA on residue at 900°C (ramp of 10°C/min in air flow)

Figure

Click here to download high resolution image

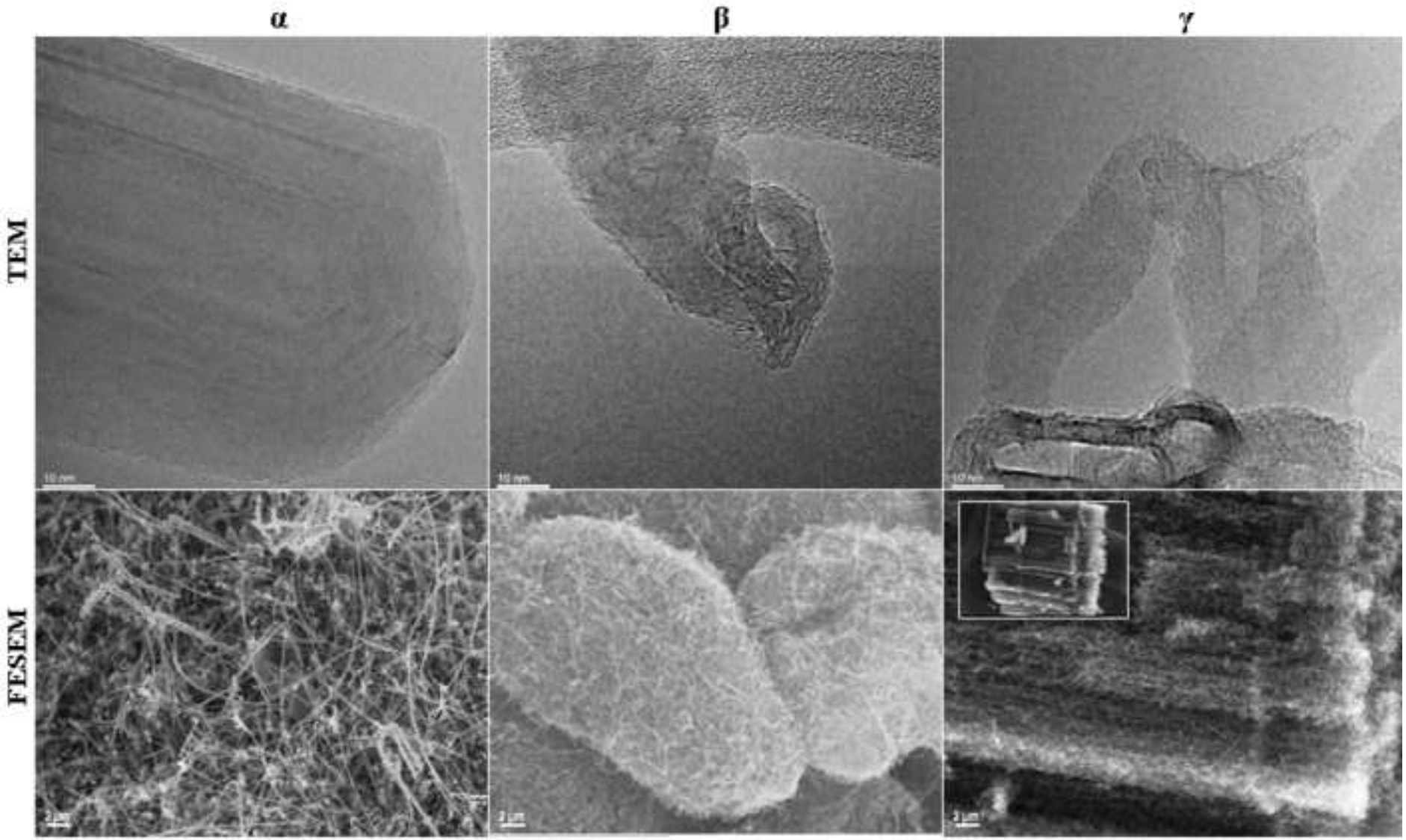

Figure

Click here to download high resolution image

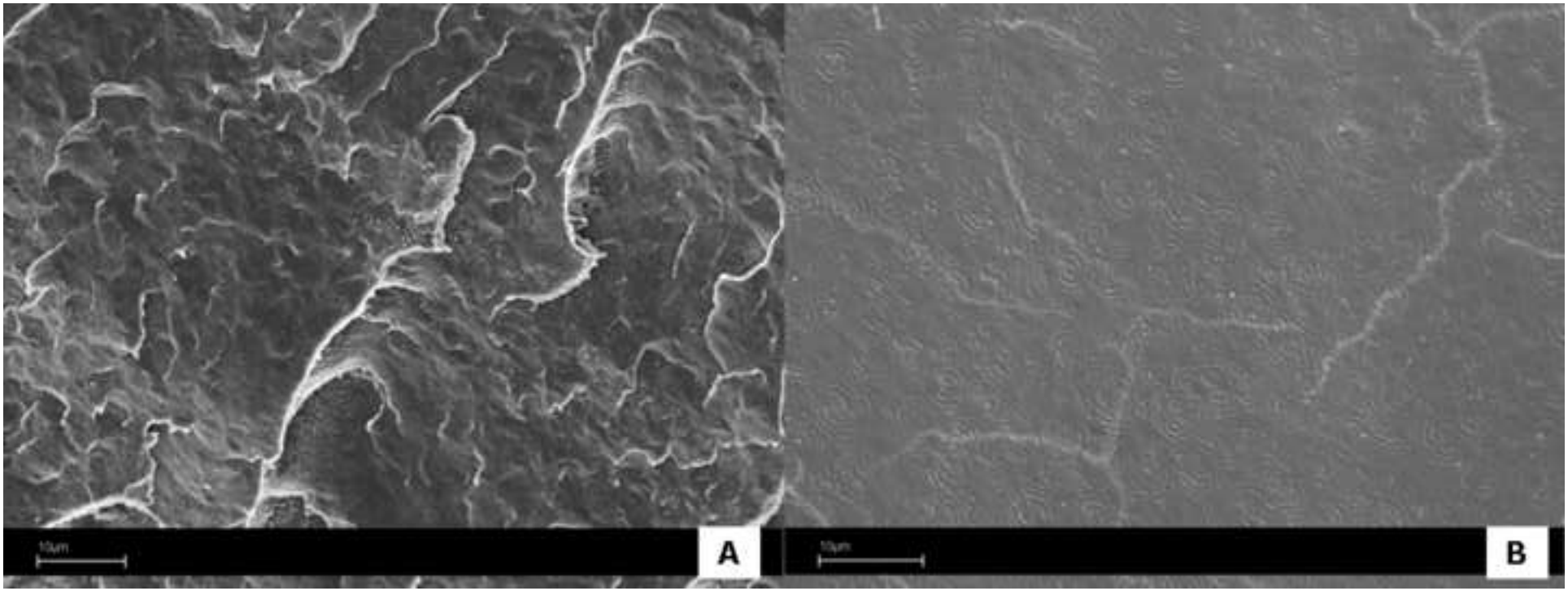

Figure

Click here to download high resolution image

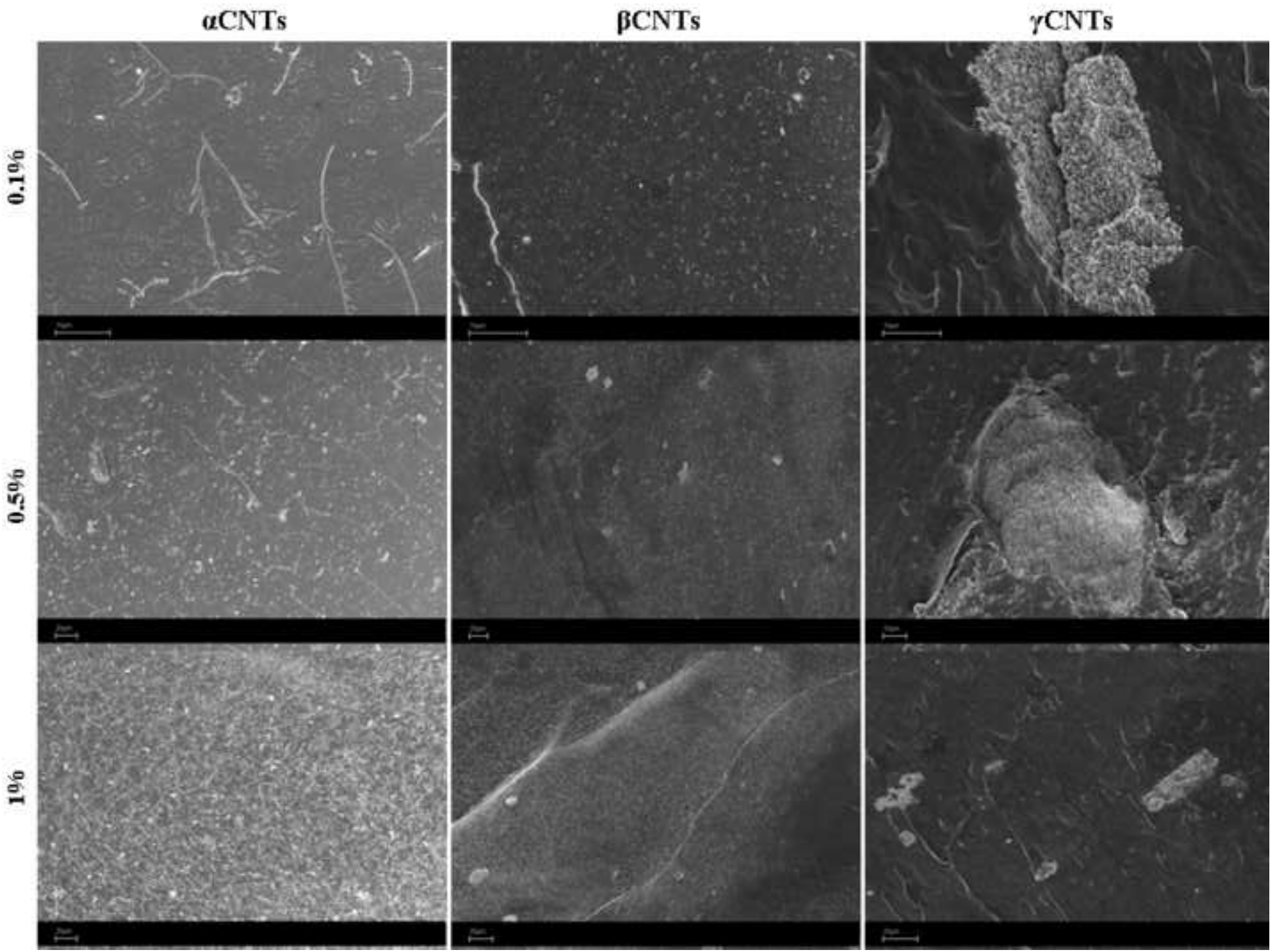

Figure 4

Click here to download high resolution image

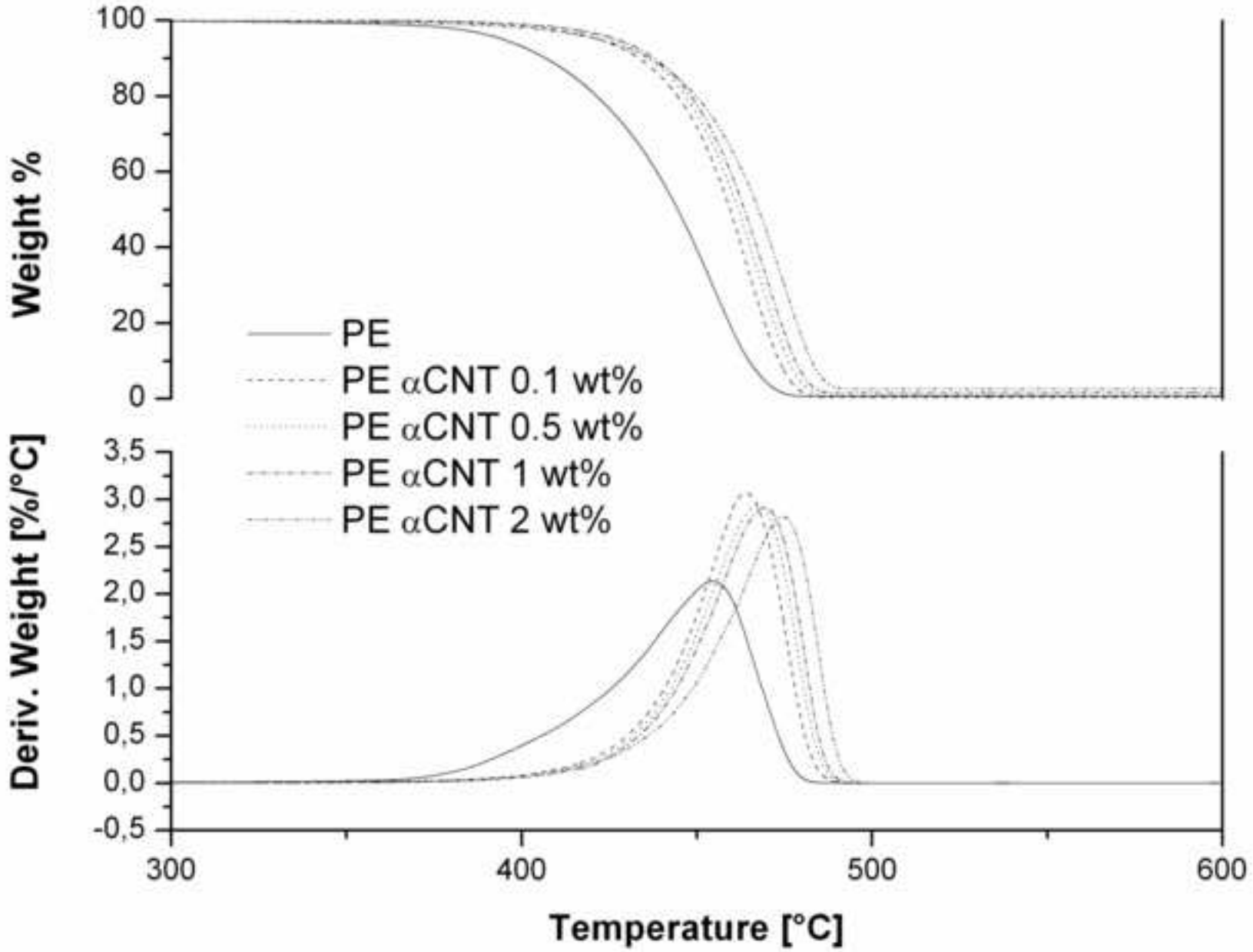

Figure 5

Click here to download high resolution image

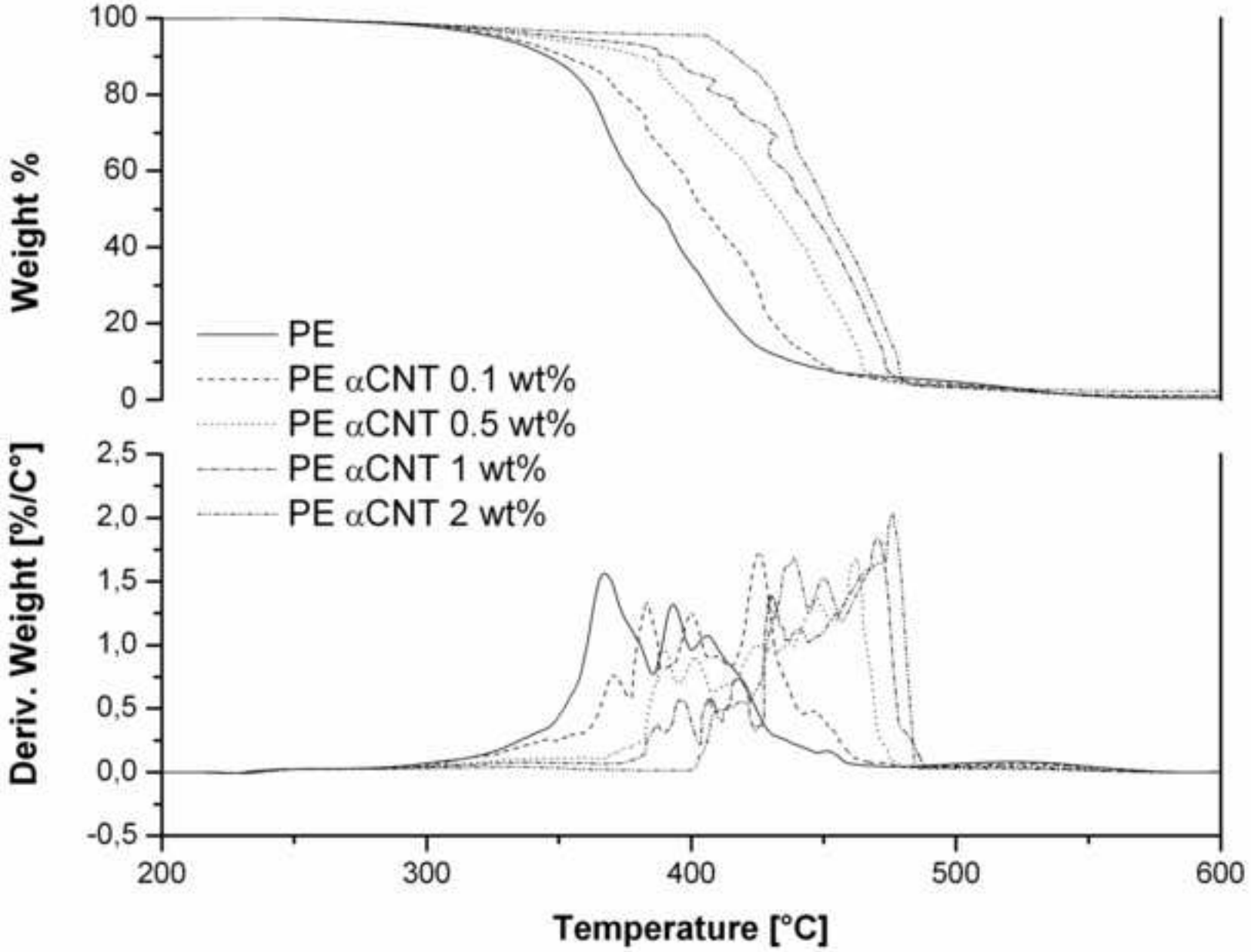

Figure 6

Click here to download high resolution image

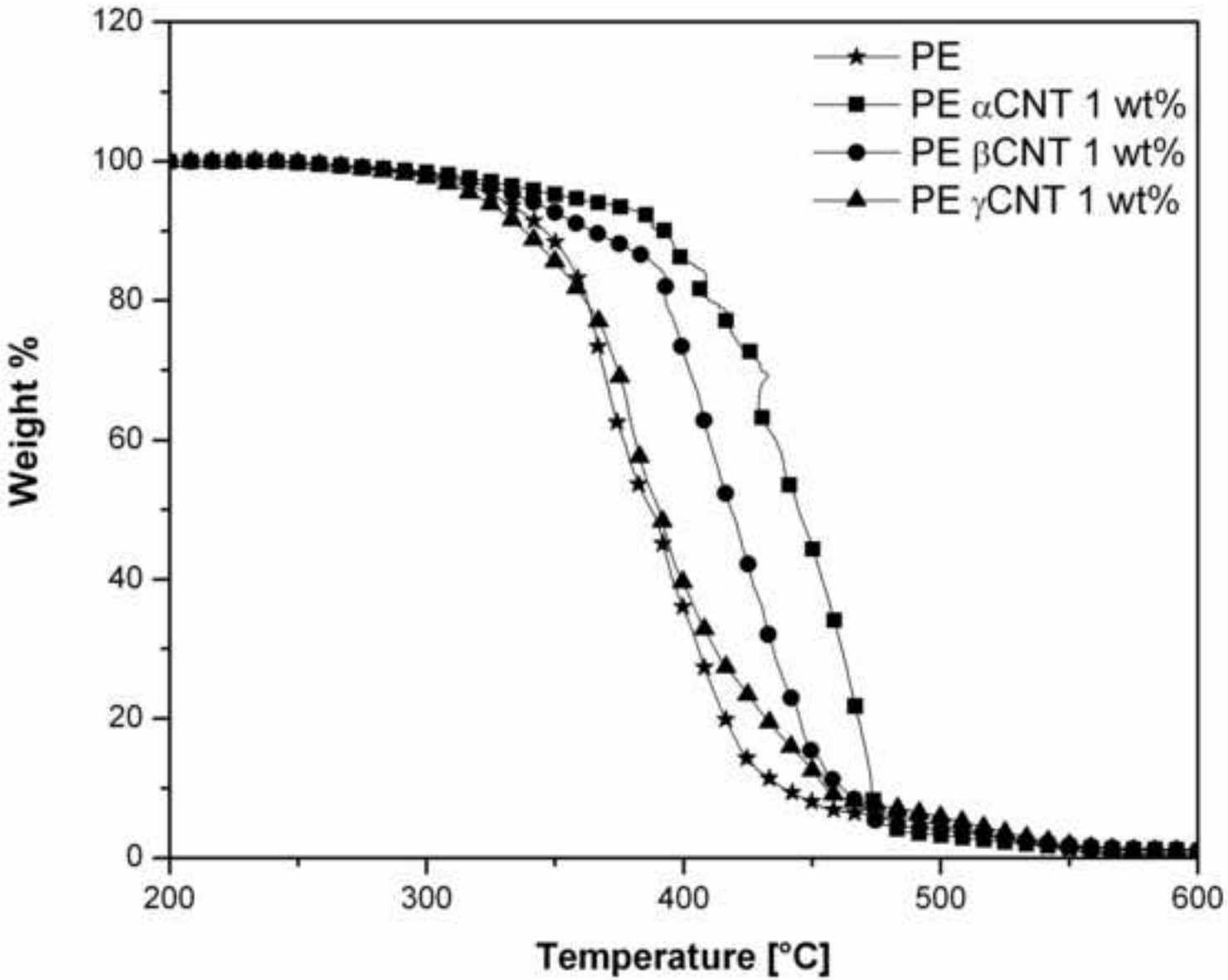

Figure 7

Click here to download high resolution image

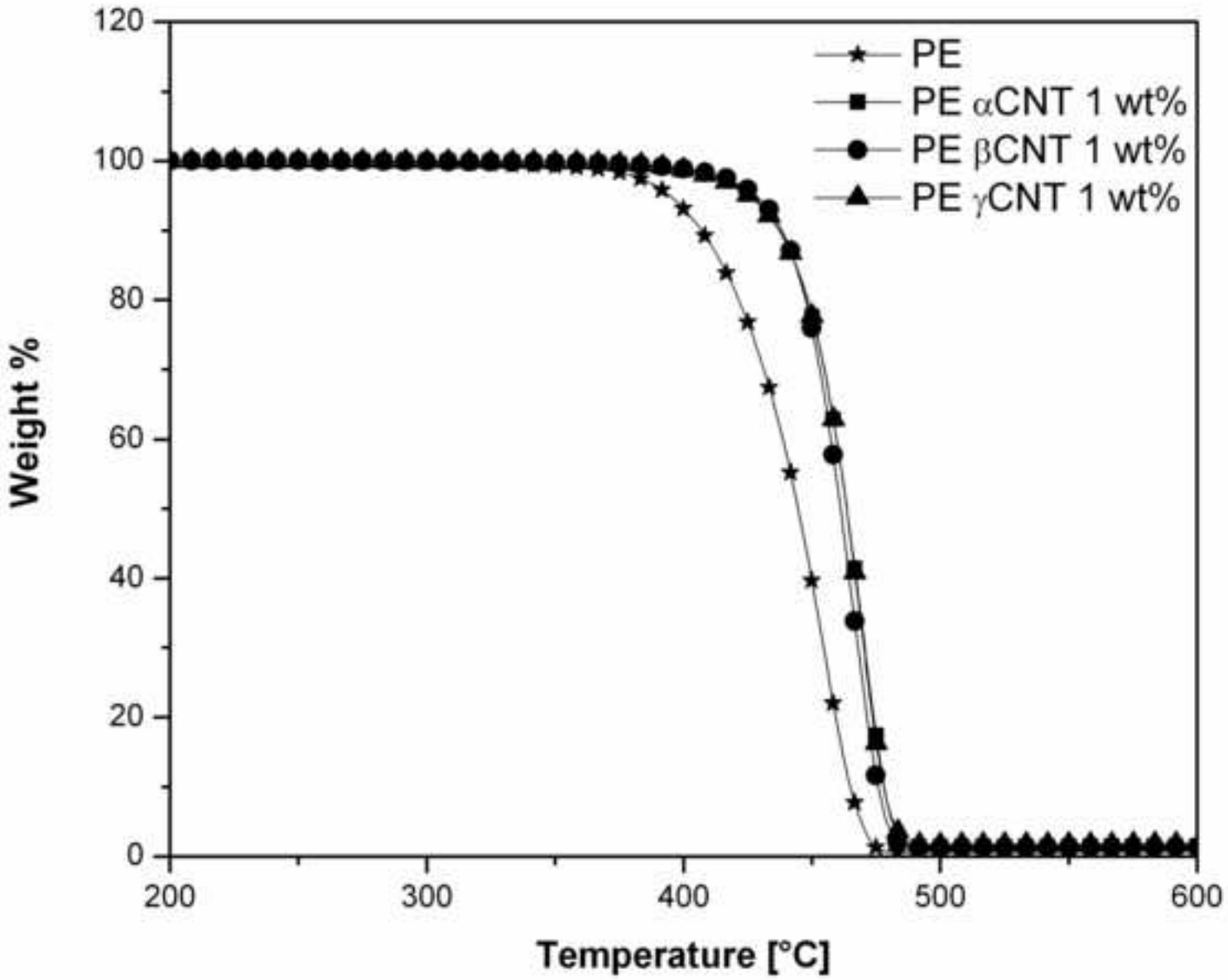

Figure 8

Click here to download high resolution image

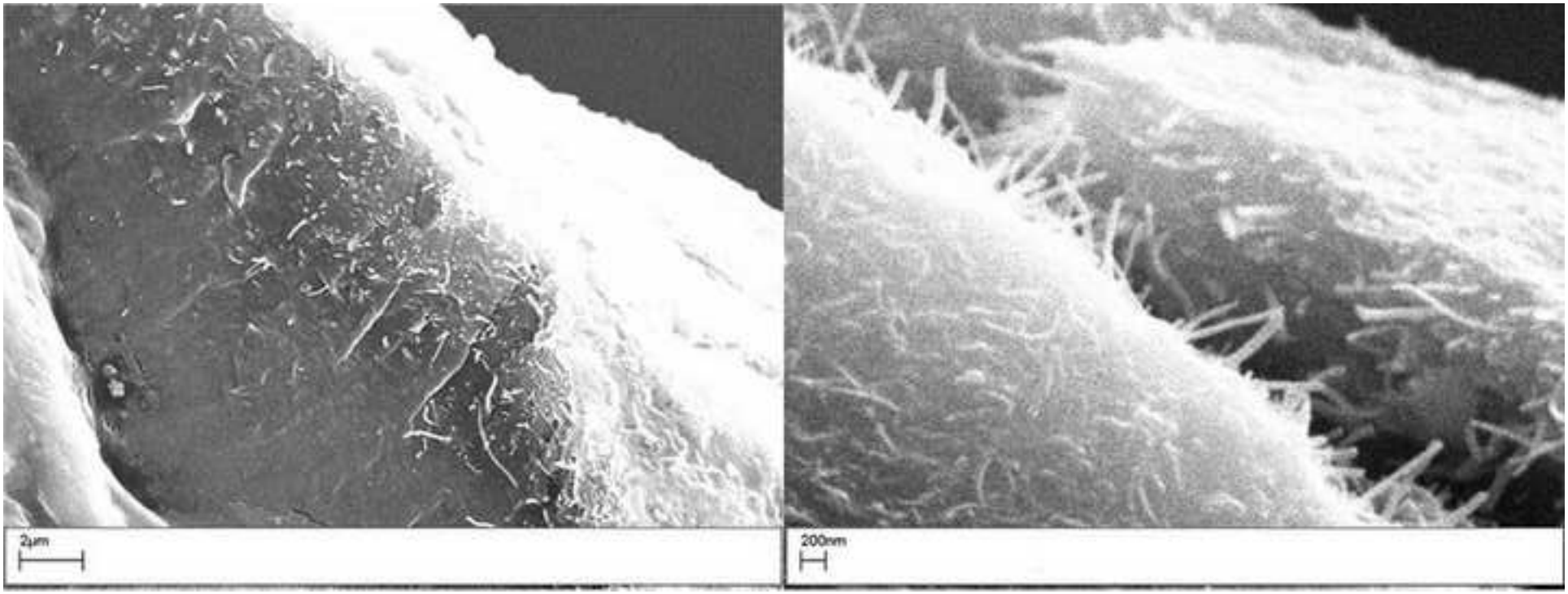

Figure 9

Click here to download high resolution image